*Desalination and Water Treatment*
www.deswater.com
doi: 10.1080/19443994.2013.782570

52 (2014) 274–282
January

Taylor & Francis
Taylor & Francis Group

# Ion-imprinted poly(2-acrylamido-2-methyl-1-propansulfonic acid)/modified silica composite hydrogel for selective and enhanced adsorption of Pb(II) ions

Jingjing Wang[a,b,*], Xianning Li[c]

[a]*School of Energy and Environment, Southeast university, Nanjing 210096, China*
[b]*Department of Polymer Materials and Engineering, School of Material Engineering, Yancheng Institute of Technology, Yancheng 224051, China*
*Email: jjwang1@hotmail.com*
[c]*School of Energy and Environment, Southeast University, Nanjing 210096, China*

Received 13 November 2012; Accepted 28 February 2013

## ABSTRACT

In this research, ion-imprinted poly(2-acrylamido-2-methyl-1-propansulfonic acid)/modified silica composite hydrogels were prepared using Pb(II) ions as template by *in situ* free-radical polymerization. The ability of the imprinted composite hydrogels to adsorb and remove Pb (II) ions from aqueous solutions was assessed using batch adsorption technique. The adsorption amount was pH-dependent, and the maximum adsorption capacity was observed at pH 5.0. The adsorption process could be well described by the Langmuir isotherm. The adsorption equilibrium was achieved within 15 min, and the kinetics of adsorption followed a pseudo-second-order rate equation. Thermodynamic parameters such as the Gibbs free energy ($\Delta G^0$), enthalpy ($\Delta H^0$), and entropy ($\Delta S^0$) for the metal ion adsorption were estimated. Results suggested that the adsorption process was a spontaneous, exothermic process that had positive entropy. The Pb(II) ion-imprinted composite hydrogels exhibited extremely high selectivity coefficient, which was much higher than that of corresponding non-imprinted composite hydrogels. Regeneration studies suggested that metal ion rebinding capacity of the Pb(II) ion-imprinted composite hydrogels did not change significantly through six cycles of sorption–desorption process.

*Keywords:* Silica; Composite hydrogel; Selective adsorption; Ion-imprinted

## 1. Introduction

The molecular or ionic imprinting technique is an approach to prepare ‘‘host’’ molecules that can recognize ‘‘guest’’ species (molecules or ions) [1]. A template molecule or ionic specie is self-assembled with the functional monomers to form a variety of bonded complexes. The complex is then polymerized in the presence of cross-linkers to produce a rigid network structure. When the templates are removed, the binding sites (cavities) are formed in the polymer matrix. As these cavities are spatially and functionally accessible to the templates, the imprinted polymers synthesized have strong selective recognition abilities toward the template molecule or ion from a mixture of chemical species [2]. In addition, molecular or ion imprinted

---

*Corresponding author.

polymers have many advantages such as easy storage, reusability, and utility in harsh environment.

During the past several years, numerous studies on ion imprinted polymers and their use for selective separation and preconcentration of metal ions have been reported, including lanthanides, actinide, noble metals, and heavy metals [3–5]. In order to remove /separate a specific metal ion from a mixture, whether toxic or precious, a selective separation method is required. Selective separation of heavy metal ions is desirable not only from an environmental standpoint but also as an economical one when the metal is precious or reusable. Lead ion, same as other heavy metal ions, has harmful effects on the ecology and living organisms. Wastewater containing lead ions brings a series of serious environmental problem because of high toxicity and accumulation in the environment. Especially, accumulation of lead ions in the human body can cause cancer and brain damage. Hence, the selective detection of lead ions is of great importance for environmental protection [6]. Among the methods for the removal of heavy metal ions, adsorption is generally preferred due to its high efficiency, easy handling, and availability of different adsorbents. Many publications concentrated on the use of hydrogels having amide, amine, carboxylic acid, or ammonium groups that can bind with heavy metal ions, as the adsorbent to remove the heavy metal ions because their high adsorption capacity, the ease of operation, especially regeneration ability encourage their applications in waste water treatment [7,8].

However, hydrogels prepared from either natural or synthetic sources usually exhibit poor mechanical properties. Generally, addition of rigid silica particles to a polymer matrix can result in an increase in the strength and modulus of the composite, because of the strong interactions or chemical bonding between silica particles and the polymer components [9].

Silica/polymer composites are promising materials that have been widely used as aerospace materials, structural materials, electronics, sensors, etc. Three main synthesis approaches have been developed to produce silica/polymer composites. The first approach involves mixing polymers with silica particles or silica precursors directly [10,11]. For example, silica composites of poly(methyl methacrylate), poly(ethylene glycol) and polyurethane have been prepared by mixing these polymers with silica colloids in solution or silica precursors that hydrolyze and condense to form silica within the polymer matrix. The second synthesis approach usually involves direct mixing of the polymer monomers with silica particles followed by polymerization of the monomers [12,13]. For example, silica colloids in solution have been mixed with organic monomers such as styrene, methyl methacrylate, ethyl acrylate, and 2-hydroxyethyl methacrylate. Subsequent polymerization of these monomers led to the formation of silica composites. The third synthesis approach involves mixing both silica precursors and polymer monomers followed by simultaneous polymerization of the precursors and monomers. Silica composites of polystyrene or poly(2-hydroxyethyl methacrylate) have been prepared using this approach [14,15].

To the best knowledge of the author, there have been no reports about the silica based ion-imprinted composite hydrogels used for selective metal ion adsorption. In this research, ion-imprinted poly(2-acrylamido-2-methyl-1-propansulfonic acid) (AMPS)/ modified silica composite hydrogels were prepared using *in situ* free-radical polymerization. At the same time, the nonimprinted composite hydrogels were synthesized as a control. The influence of pH value of the feed solution on the adsorption amount of Pb(II) ions from aqueous solutions was studied. Then, the adsorption kinetic, thermodynamic parameters and adsorption isotherm of the imprinted composite hydrogels were investigated. Finally, the selective adsorption and regeneration abilities of the imprinted composite hydrogels were evaluated.

## 2. Materials and methods

### 2.1. Materials

Silica nanoparticles (10 nm in size), and AMPS were purchased from Sigma–Aldrich Chemicals. *N,N*´-methylene bisacrylamide (MBA) and ammonium persulfate (APS), used as a cross-linking agent and an initiator, were purchased from Sigma–Aldrich Chemicals and used without further purification. Lead nitrate [$Pb(NO_3)_2{\cdot}6H_2O$] used in adsorption experiments was purchased from Shanghai Chemical Reagents Co. China. In order to improve the metal ion adsorption capacity, silica was modified by the amination reaction using the method as described in the literature [16,17]. Fig. 1 shows the chemical structure of the modified silica ($SiO_2$–$NH_2$).

### 2.2. Preparation of Pb(II) ion-imprinted composite hydrogels

The Pb(II) ion-imprinted composite hydrogel [Pb(II)-IICH] was synthesized by *in situ* free-radical poly-

Fig. 1. The structure of the modified silica ($SiO_2$–$NH_2$).

merization with MBA as a cross-linker and Pb(II) ions as the template. The detailed synthesis route was described as follows. A mixture of 1.5 g AMPS, 0.5 g $SiO_2–NH_2$, and 0.79 g $Pb(NO_3)_2·6H_2O$ were added into distilled water. And the mixture was stirred vigorously for 1 h. Then, 0.075 g MBA (5% w/w based on AMPS) and 0.015 g APS (1% w/w based on AMPS) were added into the solution as the crosslinker and initiator. The solution was heated for 24 h in a constant temperature water bath at 65℃ until the monomer AMPS polymerized completely. Then, the product was grinded and treated with 1.0 mol $L^{-1}$ HCl to completely leach Pb(II) ions. At last, the composite hydrogel was filtered with distilled water to neutralization and dried at 60℃ under vacuum, resulting in the desired Pb(II)-IICH. By comparison, the nonimprinted composite hydrogel (NICH) was similarly synthesized in the absence of $Pb(NO_3)_2·6H_2O$.

### 2.3. Adsorption capability studies

Adsorption studies were carried out in magnetically stirred (160 rpm), thermostated (25℃) cylindrical glass vessels in batch conditions. The dried composite hydrogels was added into Pb(II) ion solution (0.005 mol $L^{-1}$ metal ion, 500 mL) to determine the metal ion adsorption capacity of the samples under noncompetitive conditions. The pH of the metal feed solutions was adjusted using 0.01 mol $L^{-1}$ citrate solution before the sample was applied for the adsorption process. Amount of the residual metal ions in the solution was determined using a Thermo Elemental-X Series Inductively Coupled Plasma-Mass Spectrometer (ICP-MS) after 24 h [18]. Amount of adsorbed metal ion ($q$, mmol/g) was calculated from the following equation:

$$q = \frac{(C_0 - C)V}{m} \tag{1}$$

where $C_0$ (mmol $L^{-1}$) and $C$ (mmol $L^{-1}$) were the metal ion concentrations in the initial solution and after the adsorption for different periods of time, respectively. $V$ ($L$) was the volume of the solution added and $m$ (g) was the amount of sample used.

### 2.4. Adsorption kinetics

Batch studies were carried out using the Pb(II)-IICH to determine the effect of time duration on the chelation of Pb(II) ions at 25℃. The Pb(II)-IICH was added into the Pb(II) ion solution (0.005 mol $L^{-1}$) at pH = 5. At regular intervals, amount of adsorbed Pb(II) ions was determined as mentioned previously.

### 2.5. Equilibrium adsorption isotherm

The studies were carried out using the Pb(II)-IICH to determine the effect of the initial metal ion concentration, which varied from 0.0005 to 0.005 mol $L^{-1}$, on the adsorption capability. The pH and temperature of incubation were 5.0 and 25℃, respectively.

### 2.6. Selective adsorption studies

The selectivity of the Pb(II)-IICH and NICH for Pb (II) ions over other heavy metal ions was evaluated from the selectivity coefficient ($\beta_{Pb^{2+}/M^{2+}}$) [19], which was defined as:

$$\beta_{Pb^{2+}/M^{2+}} = \frac{D_{Pb^{2+}}}{D_{M^{2+}}} \tag{2}$$

where $D_{Pb}^{2+}$ and $D_{M}^{2+}$ were the distribution ratios of the Pb(II) ions and other coexistent heavy metal ions, respectively. The distribution ratio ($D$) was calculated by using the following expression:

$$D = \frac{C_0 - C_e}{C_e} \times \frac{V}{W} \tag{3}$$

where $C_0$ and $C_e$ were the concentrations of metal ions in the initial solution and equilibrium solution (mol $L^{-1}$), respectively, and $V$ was the volume of the aqueous solution ($L$) and $W$ was the mass of dry composite hydrogels (g).

The effect of imprinting on selective adsorption was evaluated with the relative selectivity coefficient $\beta_r$, which can be defined as the following expression:

$$\beta_r = \frac{\beta_{imprinted}}{\beta_{non\text{-}imprinted}} \tag{4}$$

where $\beta_{imprinted}$ and $\beta_{non\text{-}imprinted}$ were selectivity coefficients of the imprinted and non-imprinted composite hydrogels, respectively.

### 2.7. Regeneration studies

The metal ions were freed from the metal-complexed Pb(II)-IICH by treating with 1 mol $L^{-1}$ HCl. The acid-treated Pb(II)-IICH was filtered and washed with distilled water to remove acid. The concentration of desorbed metals was determined as mentioned above. The desorption ratio was calculated as follows: desorption ratio = (Amount of metal ion desorbed into solution/ Amount of metal ion bound to Pb(II)-IICH) × 100%. A second metal binding cycle was repeated with the regenerated Pb(II)-IICH. Recovery ratio = (Amount of

Pb(II) ion adsorbed in the second run/Amount of Pb(II) ion adsorpted in the first run) × 100%.

## 3. Results and discussion

### 3.1. Adsorption studies

Metal ion sorption on sorbent is influenced by pH due to the competition between the metal and $H^+$ ions for active sorption sites, so the pH value is one of the important factors controlling the sorption of Pb(II) ions from aqueous solutions. The distribution of metal species in aqueous solution as a function of pH reveals that Pb(II) ions precipitate in the forms of metal oxides or hydroxides at $pH > 6$. Hence, the experiments were conducted at $pH = 2$, 3, 4, and 5. In this case, the sorption, not precipitation, was responsible for the removal of Pb(II) ions [20].

Fig. 2 shows the effect of pH on the adsorption of Pb(II) ions by imprinted and nonimprinted composite hydrogels. It could be seen that the adsorption capacity for both composite hydrogels increased remarkably with increasing pH values and reached to maximum at pH 5.0. The highest adsorption amount for Pb(II) ions onto Pb(II)-IICH and NICH were 13.45 and 7.58 mmol $g^{-1}$, respectively, from which the imprinting effect was clearly observed. The adsorption capacity for Pb(II)-IICH was higher than that for NICH at all pH values because in Pb(II)-IICH the cavities created after removal of template were complementary to the imprint ion in size and coordination geometries, whereas in NICH there was a random distribution of ligand functionalities.

As expected, due to the involvement of $-NH_2$ group in complexation with Pb(II) ions, the sorption of Pb(II) ions at lower pH values was highly dependent on the pH of solution, because of the competition of proton with Pb(II) ions for $-NH_2$ site. Therefore, smaller amount of Pb(II) ions was adsorbed by the Pb(II)-IICH. As the pH increased, the protonation of ligand was suppressed, resulting in more favorable for complex formation and sorption of Pb(II) ions to the composite hydrogels. The adsorption capacity above pH 5.0 was not investigated because of the possibility of hydrolysis and precipitation of the Pb(II) ions.

### 3.2. Adsorption kinetics

Fig. 3 shows the time dependence of adsorption capacity of Pb(II) ions on Pb(II)-IICH. High adsorption rate was observed at the beginning of the adsorption process, after which adsorption equilibrium was quickly reached within 15 min. The maximum adsorption capacity for Pb(II) ions was 13.45 mmol $g^{-1}$ of dry Pb(II)-IICH. This fast adsorption equilibrium was probably due to high complexation rate and geometric shape affinity (or memory) between Pb(II) ions and Pb(II) cavities in the composite hydrogel structure. It was well known that removal of the template from the Pb(II)-IICH matrix leaved cavities of complementary size, shape, and chemical functionality to the template. This template effect was attributed to the existence of Pb(II) ion memorized cavities on the hydrogel surface [21]. A desirable coordination space was formed on the surfaces to facilitate the interaction with the adsorbed Pb (II) ions.

For evaluating the adsorption kinetic of Pb(II) ions on Pb(II)-IICH, the kinetic data were fitted by the pseudo-first-order and pseudo-second-order kinetic models [22], which were respectively expressed as follows:

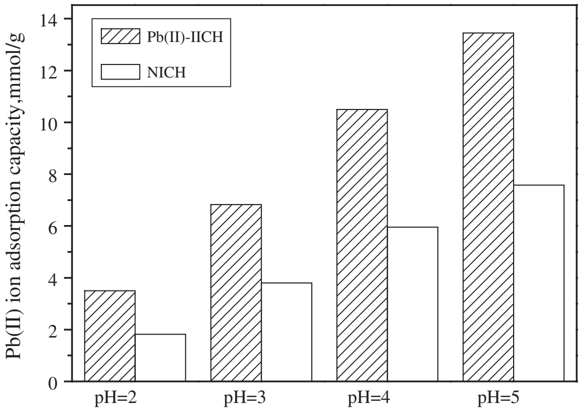

Fig. 2. Influence of pH values on the adsorption capacity of Pb(II)-IICH and NICH.

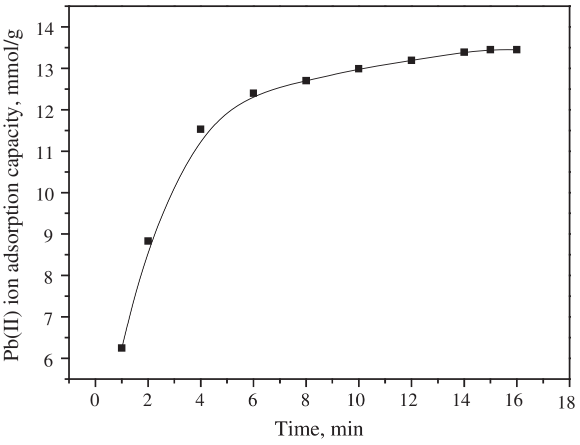

Fig. 3. The time dependence of adsorption capacity of Pb(II) ions by the Pb(II)-IICH.

$$\ln(q_e - q_t) = \ln q_e - k_1 t \tag{5}$$

$$\frac{t}{q_t} = \frac{1}{k_2 q_e^2} + \frac{t}{q_e} \tag{6}$$

where $t$ was the contact time (min); $q_t$ and $q_e$ were the amount of Pb(II) ions adsorbed at an arbitrary time $t$ and at equilibrium (mmol g$^{-1}$), respectively; $k_1$ (min$^{-1}$) and $k_2$ (g mmol$^{-1}$ min$^{-1}$) were the rate constants of adsorption, respectively.

The plot of ln($q_e$−$q_t$) vs. $t$, and $t/q_t$ vs. $t$ for the adsorption of Cu(II) ions were respectively shown in Figs. 4 and 5. The results showed that the correlation coefficient for the pseudo-first-order kinetic model was relatively low ($R^2 = 0.972$). However, the pseudo-second-order rate equation for the adsorption of Cu (II) ions onto Pb(II)-IICH agreed well with the data ($R^2 = 0.999$). Based on the correlation coefficient, the pseudo-second-order rate equation was fairly suited to depict the adsorbing kinetic process of Pb(II) ions on Pb(II)-IICH, suggesting chemical sorption as the rate-limiting step of the adsorption process [22].

### 3.3. Adsorption isotherms

Adsorption isotherms were used to evaluate the adsorption properties of the Pb(II)-IICH. Fig. 6 shows the dependence of the equilibrium concentration on the adsorbed amount of Pb(II) ions onto the composite hydrogels with the initial Pb(II) ion concentration ranging from 0.0005 to 0.005 mol L$^{-1}$. It was evident that the adsorption capacity increased with the initial concentration of Pb(II) ion in solution, progressively saturating the adsorbent. That was satisfactory for the trace analysis of Pb(II) ions in aqueous solutions.

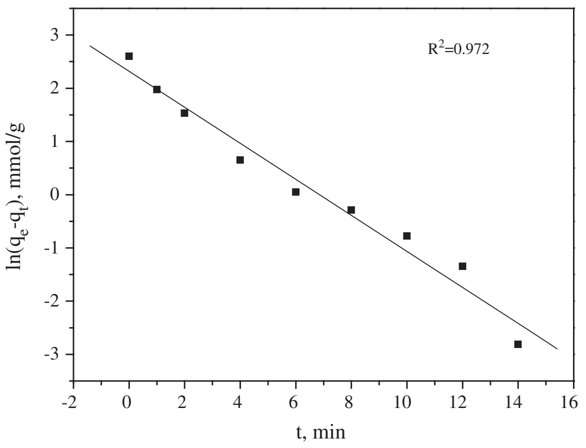

Fig. 4. Pseudo-first-order kinetic for adsorption of Pb(II) ions by the Pb(II)-IICH.

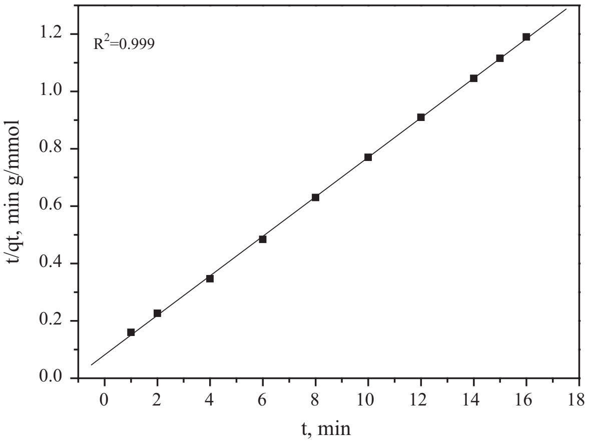

Fig. 5. Pseudo-second-order kinetic for adsorption of Pb(II) ions by the Pb(II)-IICH.

Equilibrium data, commonly known as adsorption isotherm, are basic requirements for designing of adsorption systems. In this work, the equilibrium data for Pb(II) ions on Pb(II)-IICH were modeled with the Langmuir and Freundlich isotherm equation in the linearized form [23], which were respectively expressed as follows:

$$\frac{C_e}{q_e} = \frac{K}{q_m} + \frac{C_e}{q_m} \tag{7}$$

$$\ln\ q_e = \frac{1}{n}\ln\ C_e + \ln K_F \tag{8}$$

where $q_e$ was the equilibrium metal ion adsorption amount (mol g$^{-1}$), $C_e$ was the equilibrium metal ion

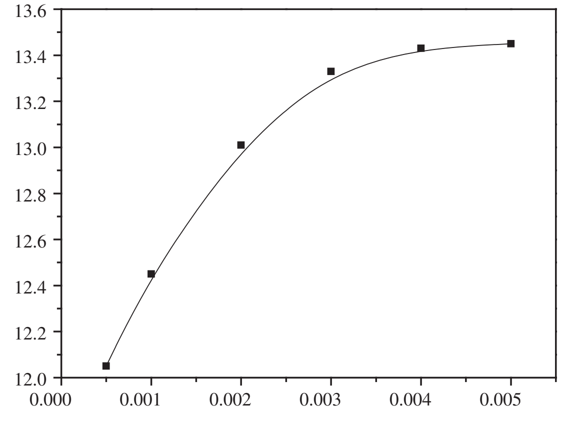

Fig. 6. Adsorption capacity for Pb(II) ions at various concentrations on the Pb(II)-IICH at pH = 5.

concentration in the solution ($\text{mol L}^{-1}$), $q_m$ represented the maximum amount of metal ions that could be adsorbed on the Pb(II)-IICH ($\text{mol g}^{-1}$), and $K$ was a constant of the Langmuir model ($\text{mol L}^{-1}$). $K_F$ ($\text{mol g}^{-1}$) and $n$ were the Freundlich constants depicting the adsorption process.

The plot of $C_e/q_e$ against $C_e$ and $\ln q_e$ vs. $\ln C_e$ for the experimental data were respectively shown in Figs. 7 and 8. The adsorption of Pb (II) on Pb(II)-IICH was well fitted to the Langmuir isotherm model ($R^2 = 0.9999$). However, the correlation coefficient of Freundlich isotherm model was low ($R^2 = 0.9781$). The theoretical $q_m$ value (13.68 $\text{mmol g}^{-1}$) calculated from the Langmuir adsorption model was close to the experimental value (13.45 $\text{mmol g}^{-1}$). As a result, the Langmuir adsorption model, which was considered to be the formation of monolayer coverage of analytes at the surface of the sorbent, can be applied in the adsorption process of Pb(II) onto Pb(II)-IICH [23].

### 3.4. Thermodynamic study

Thermodynamic parameters for the Pb(II) ion adsorption on Pb(II)-IICH such as Gibbs free energy ($\Delta G^0$), enthalpy ($\Delta H^0$) and entropy ($\Delta S^0$) were investigated.

The Gibbs free energy change $\Delta G^0$ could indicate the degree of the spontaneity of the adsorption process. For significant adsorption to occur, the free energy changes ($\Delta G^0$) of adsorption must be negative. The values of the standard Gibbs free energy were estimated using the following equation:

$$\Delta G^0 = -RT \ln K \tag{9}$$

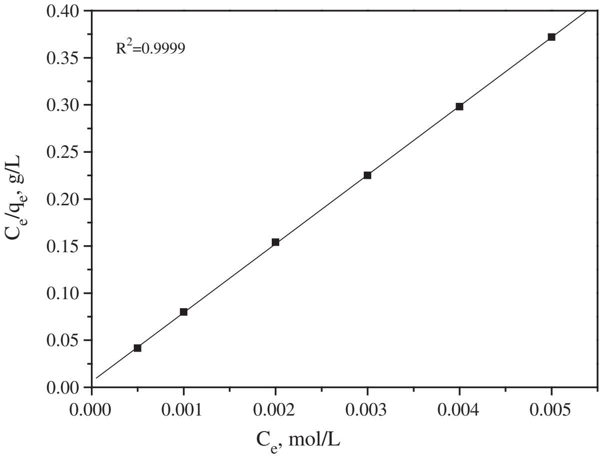

Fig. 7. Illustration of the experimental adsorption isotherm data presented in terms of the linearized Langmuir model.

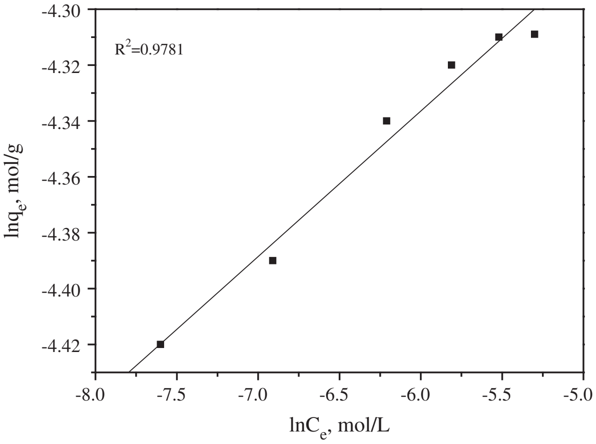

Fig. 8. Illustration of the experimental adsorption isotherm data presented in terms of the linearized Freundlich model.

where $R$ was the universal gas constant (8.314 $\text{J mol}^{-1}\,\text{K}^{-1}$) and $T$ was the Kelvin temperature. $K$ was the thermodynamic equilibrium constant for the adsorption process. It was determined using the method of Wu and Yu [24] by plotting ln ($q_e/C_e$) vs. $q_e$ and extrapolating to zero $q_e$ as suggested (Fig. 9).

Adsorption equilibrium constant $K$ for varying temperatures have been used to evaluate the thermodynamic parameters of this adsorption process, and all the thermodynamic parameters of the adsorption process are shown in Table 1. It was clear that the equilibrium constant $K$ decreased with increasing temperature above 298 K. This suggested this adsorption process was exothermic.

The negative values of free energy change ($\Delta G^0$) indicated that this adsorption process was spontaneous in nature whereby no energy input from outside of the system was required. The higher negative value reflected a more energetically favorable adsorption [25]. The Gibbs free energy value at 318 K was the highest negative value than the values of other temperatures. For that reason more energetically favorable adsorption occurred at 318 K.

The enthalpy change upon adsorption can be calculated from the following equation:

$$\ln K = \frac{-\Delta H^0}{RT} + \text{constant} \tag{10}$$

Therefore, the plot of ln $K$ vs. 1/T gave a straight line whose slope was equal to $-\Delta H^0/R$ (Fig. 10). The negative value of $\Delta H^0$ ($-159.1\ \text{kJ mol}^{-1}$) as shown in Table 1 suggested that the adsorption was exothermic and the adsorption process was enthalpically favored.

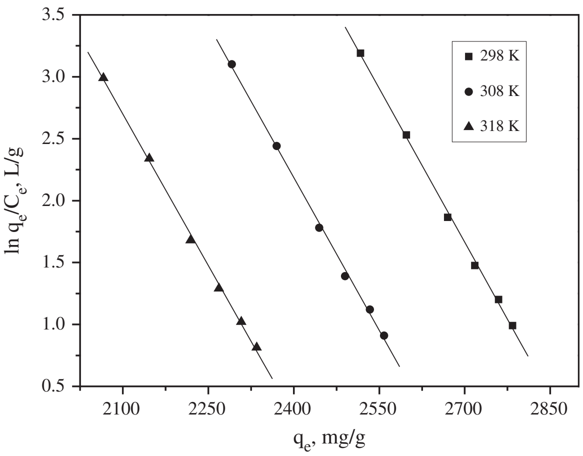

Fig. 9. Plots of $\ln(q_e/C_e)$ as a function of $q_e$ for the adsorption of Pb(II) ions by the Pb(II)-IICH.

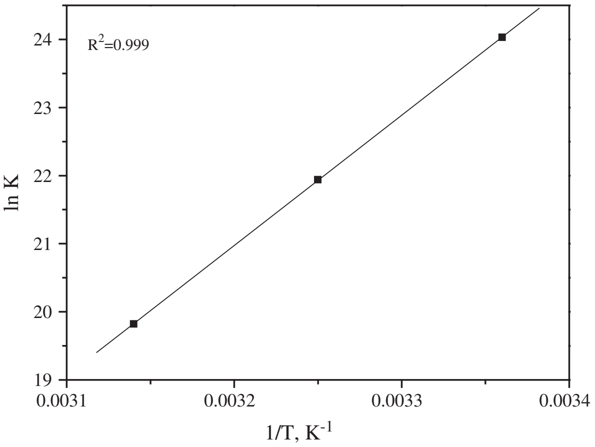

Fig. 10. Plot of $\ln K$ vs. $1/T$ for Pb(II) adsorption by the Pb (II)-IICH.

Table 1
Thermodynamic parameters of the Pb(II) ion adsorption onto the Pb(II)-IICH

| Temperature | $K$ | $\Delta G^0$ (kJ mol$^{-1}$) | $\Delta H^0$ (kJ mol$^{-1}$) | $\Delta S^0$ (J mol$^{-1}$ K) |
|---|---|---|---|---|
| 298 K | $2.73 \times 10^{10}$ | −59.536 | −159.1 | 334.11 |
| 308 K | $3.38 \times 10^{9}$ | −56.182 | | 334.15 |
| 318 K | $4.05 \times 10^{8}$ | −52.401 | | 335.53 |

The standard change in entropy can be calculated from the following equation:

$$\Delta S^0 = \frac{\Delta H^0 - \Delta G^0}{T} \tag{11}$$

The positive values of $\Delta S^0$ indicated the increased randomness at the Pb(II)-IICH/solution interface during the adsorption of metal ions onto the composite hydrogel [26].

### 3.5. Selectivity studies

The selectivity of the Pb(II)-IICH and NICH for Pb(II) ions was investigated by binding Pb(II) ions in the presence of various competitor metal ions. As shown in Table 2, the *D* values of Pb(II)-IICH increased for Pb(II) but decreased significantly for other ions. Ni(II), with a smaller ionic radius (69 pm) than Cu(II) (71 pm), Zn(II) (74 pm) and Cd (92 pm), could enter into the imprinting sites easier than Cu (II), Zn(II) and Cd(II) and thus showed higher *D* value. The explanation was supported by comparing *D* values of Pb(II)-IICH with those of NICH, which had random functional sites. The relative selectivity coefficient was an indicator to express the adsorption affinity of recognition sites to the imprinted Pb(II) ions. From the results in Table 2, the relative selectivity coefficients of imprinted composite hydrogels for Pb(II)/Ni(II), Pb(II)/Cu(II), Pb(II)/Zn(II), and Pb(II)/Cd(II) were 6.85, 6.86, 6.72, and 6.79 times greater than that of the nonimprinted composite hydrogels, respectively. These results indicated that the functional host molecules (memorized cavities) on the Pb (II)-IICH surfaces were immobilized with the strict configuration suitable for Pb(II) ions, and that the ionic recognition was influenced by the nature of metal ion, and its ionic radius and charge.

### 3.6. Regeneration studies

Under strong acid conditions, the coordination interaction of chelated Pb(II) ions could be easily disrupted and subsequently Pb(II) ions were released into the desorption medium. In the present study, 1.0 mol L$^{-1}$ HCl was used as the desorption reagent for elution of Pb(II) ions. It could be observed that Pb (II) ions could be quantitatively eluted with desorption ratio >98%.

In order to examine the reusability of the prepared Pb(II)-IICH, the experiments (sorption/desorption cycle) were repeatedly performed by using the same sample. The sorption/desorption cycles were conducted six times. From the obtained results summarized in Table 3,

Table 2
Selective separation property of Pb(II)-IICH and NICH

| Ions | Ionic charge | Ionic radii (pm) | Distribution ratio, mL $g^{-1}$ | | Selectivity coefficient $\beta_{\mathrm{CU}^{2+}/\mathrm{M}^{2+}}$ | | Relative selectivity coefficient $\beta_r$ |
|---|---|---|---|---|---|---|---|
| | | | Pb(II)-IICH | NICH | Pb(II)-IICH | NICH | |
| Pb(II) | 2 | 120 | 3,842 | 550 | – | – | – |
| Ni(II) | 2 | 69 | 510 | 502 | 7.53 | 1.10 | 6.85 |
| Cu(II) | 2 | 71 | 496 | 485 | 7.75 | 1.13 | 6.86 |
| Zn(II) | 2 | 74 | 480 | 464 | 8.00 | 1.19 | 6.72 |
| Cd(II) | 2 | 92 | 413 | 402 | 9.30 | 1.37 | 6.79 |

Table 3
The effect of reused times on the adsorption capacity of Pb(II)-IICH

| Reused times | 1 | 2 | 3 | 4 | 5 | 6 |
|---|---|---|---|---|---|---|
| Adsorption capacity (mmol $g^{-1}$) | 13.05 | 13.00 | 12.93 | 12.86 | 12.80 | 12.78 |
| Recovery ratio (%) | 97.03 | 96.65 | 96.13 | 95.61 | 95.17 | 95.02 |

it could be seen that the affinity of Pb(II)-IICH remained unchanged although it underwent six cycles of sorption/desorption process.

## 4. Conclusion

Ion-imprinted poly(AMPS)/modified silica composite hydrogels were prepared using Pb(II) ions as template by *in situ* free-radical polymerization. The composite hydrogels were used to remove Pb(II) ions from aqueous solution under the noncompetitive condition. The results showed that the adsorption capacity of the composite hydrogels increased with the pH values. High adsorption rate was observed at the beginning of the adsorption process, after which adsorption equilibrium was quickly reached within 15 min. The adsorption capacity increased with the initial concentration of Pb(II) ion in solution, and the adsorption data could be well fitted by the Langmuir isotherm. The investigation of the thermodynamic parameters indicated that the adsorption process was a spontaneous, exothermic process that had positive entropy. The relative selectivity coefficients of imprinted composite hydrogels for Pb(II)/Ni(II), Pb(II)/Cu(II), Pb(II)/Zn(II), and Pb(II)/Cd(II) were 6.85, 6.86, 6.72, and 6.79 times greater than that of the nonimprinted composite hydrogels, respectively, indicating that the Pb(II) ion-imprinted composite hydrogels had strong adsorption selectivity for Pb(II) ion. Regeneration studies suggested that metal rebinding capacity of the ion-imprinted composite hydrogels did not change significantly through six cycles of sorption/desorption process.

## Acknowledgments

This Project was supported by China Postdoctoral Science Foundation (No. 2012M520979) and Jiangsu Postdoctoral Science Foundation (No. 1201009B).

## References

[1] L. Donato, M.C. Greco, E. Drioli, Preparation of molecularly imprinted membranes and evaluation of their performance in the selective recognition of dimethoate, Desalin. Water Treat. 30 (2011) 171–177.

[2] N.T. Hoai, D. Kim, Synthesis, structure, and selective separation behavior of copper-imprinted microporous polymethacrylate beads, AIChE J. 55 (2009) 3248–3254.

[3] A. Jayalakshmi, S. Rajesh, S. Senthilkumar, D. Mohan, Epoxy functionalized poly(ether-sulfone) incorporated cellulose acetate ultrafiltration membrane for the removal of chromium ions, Sep. Purif. Technol. 90 (2012) 120–132.

[4] N.T. Hoai, D.K. Yoo, D. Kim, Batch and column separation characteristics of copper-imprinted porous polymer microbeads synthesized by a direct imprinting method, J. Hazard. Mater. 173 (2010) 462–467.

[5] D.K. Singh, S. Mishra, Synthesis and characterization of Hg(II)-ion-imprinted polymer: Kinetic and isotherm studies, Desalination 257 (2010) 177–183.

[6] Y. Liu, Z. Liu, Y. Wang, J. Dai, J. Gao, J. Xie, Y. Yan, A surface ion-imprinted mesoporous sorbent for separation and determination of Pb(II) ion by flame atomic absorption spectrometry, Microchim. Acta 172 (2011) 309–317.

[7] T.S. Anirudhan, S. Rijith, V.R.N. Ratheesh, A highly efficient carboxyl-terminated hybrid adsorbent composite matrix for the adsorption of uranium(VI) and thorium(IV) from aqueous solutions and nuclear industry effluents, Desalin. Water Treat. 38 (2012) 79–89.

[8] M.R. Guilherme, A.V. Reis, A.T. Paulino, T.A. Moia, L.H.C. Mattoso, E.B. Tambourgi, Pectin-based polymer hydrogel as a carrier for release of agricultural nutrients and removal of heavy metals from wastewater, J. Appl. Polym. Sci. 117 (2010) 3146–3154.

[9] Y. Ou, F. Yang, Z. Yu, A new conception on the toughness of nylon 6/silica nanocomposite prepared via *in situ* polymerization, J. Polym. Sci., Part B: Polym. Phys. 36 (1998) 789–795.

[10] Z.S. Petrovic, I. Javni, A. Waddon, G. Banhegyi, Structure and properties of polyurethane-silica nanocomposites, J. Appl. Polym. Sci. 76 (2000) 133–151.

[11] M. Laridjani, E. Lafontaine, J.P. Bayle, P. Judeinstein, Structural studies of ideal organic–inorganic nanocomposites by high resolution diffractometry and NMR spectroscopy techniques, J. Mater. Sci. 34 (1999) 5945–5953.

[12] M.J. Percy, C. Barthet, J.C. Lobb, M.A. Khan, S.F. Lascelles, M. Vamvakaki, S.P. Armes, Synthesis and characterization of vinyl polymer-silica colloidal nanocomposites, Langmuir 16 (2000) 6913–6920.

[13] M.J. Percy, S.P. Armes, Surfactant-Free synthesis of colloidal poly(methyl methacrylate)/ailica nanocomposites in the absence of auxiliary comonomers, Langmuir 18 (2002) 4562–4565.

[14] D. Kawashima, T. Aihara, Y. Kobayashi, T. Kyotani, A. Tomita, Preparation of mesoporous carbon from organic polymer/silica nanocomposite, Chem. Mater. 12 (2000) 3397–3401.

[15] G.H. Hsiue, W.J. Kuo, Y.P. Huang, R.J. Jeng, Microstructural and morphological characteristics of PS-$SiO_2$ nanocomposites, Polymer 41 (2000) 2813–2825.

[16] K. Suzuki, S. Siddiqui, C. Chappell, J.A. Siddiqui, R.M. Ottenbrite, Modification of porous silica particles with poly (acrylic acid), Polym. Adv. Technol. 11 (2000) 92–97.

[17] J.S. Kim, J. Yi, Selective removal of copper ions from multicomponent aqueous solutions using modified silica impregnated with LIX 84, J. Chem. Technol. Biotechnol. 75 (2000) 359–362.

[18] H. Kaşgöz, A. Durmus, A. Kaşgöz, Enhanced swelling and adsorption properties of AAm-AMPSNa/clay hydrogel nanocomposites for heavy metal ion removal, Polym. Adv. Technol. 19 (2008) 213–220.

[19] D.K. Singh, S. Mishra, Synthesis and characterization of $UO_2^{2+}$-ion imprinted polymer for selective extraction of $UO_2^{2+}$, Anal. Chim. Acta 644 (2009) 42–47.

[20] J.P. Chen, L. Yang, Chemical modification *Sargassum* sp. For prevention of organic leaching and enhancement of uptake during metal biosorption, Ind. Eng. Chem. Res. 44 (2005) 9931–9942.

[21] A.H. Dam, D. Kim, Metal ion-imprinted polymer microspheres derived from copper methacrylate for selective separation of heavy metal ions, J. Appl. Polym. Sci. 108 (2008) 14–24.

[22] M. Najafi, Y. Yousefi, A.A. Rafati, Synthesis, characterization and adsorption studies of several heavy metal ions on amino-functionalized silica nano hollow sphere and silica gel, Sep. Purif. Technol. 85 (2012) 193–205.

[23] S. Chatterjee, S.H. Woo, The removal of nitrate from aqueous solutions by chitosan hydrogel beads, J. Hazard. Mater. 164 (2009) 1012–1018.

[24] J. Wu, H.Q. Yu, Biosorption of 2,4-dichlorophenol from aqueous solution by phanerochaete chrysosporium biomass: isotherms, kinetics and thermodynamics, J. Hazard. Mater. 137 (2006) 498–508.

[25] Z. Aksu, E. Kabasakal, Batch adsorption of 2,4-dichlorophenoxy-acetic acid (2–4-D) from aqueous solution by granular activated carbon, Sep. Purif. Technol. 35 (2004) 223–240.

[26] M. Mahramanlioğlu, S.I. Kirbasalar, I. Kizilcikil, Mass transfer and adsorption kinetics during the adsorption of fluoride onto activated clays in agitated systems, Fresenius Environ. Bull. 12 (2003) 1483–1491.